JOURNAL OF MATERIALS SCIENCE 21 (1986) 277–283

Effects of relaxation and phase transition on the resistivity of chemically deposited $Ni_{66}B_{34}$ layers

C. R. PICHARD, A. J. TOSSER, F. A. KUHNAST*, F. MACHIZAUD*, J. FLECHON*, H. ZANTOUT
Laboratoire d'Electronique, Université de Nancy-1, BP 239, 54506 Vandoeuvre les Nancy Cedex, France
**Laboratoire de Physique des Dépôts Métalliques, Université de Nancy-1, BP 239, 54506 Vandoeuvre les Nancy Cedex, France*

The effects of thermal treatment on the conductivity and the temperature coefficient of resistivity of thin amorphous layers of Ni–B metallic glasses (66% Ni, 34% B) are analysed in terms of the dependence on thickness and ageing temperature. The layer exhibits a macroscopical structure consisting of clusters in an amorphous medium; it is assumed that the cluster resistivity is temperature independent, up to 350° C, and that the amorphous medium is altered markedly by the ageing processes. These consequences are deduced which are in agreement with a previously proposed model for a layer structure.

1. Introduction

Previous experimental data [1] related to amorphous $Ni_{66}B_{34}$ layers, chemically deposited, have led to the following results [1, 2]: (a) the film structure is continuous for film thicknesses greater than 45 nm, (b) no Fuchs–Sondheimer effect [3, 4] occurs, and (c) the product of the film resistivity, ϱ_f, with its temperature coefficient, β_f, takes a constant value for amorphous layers, provided that the layer is more than 10^2 nm thick and the ageing temperature, T_R, does not exceed 300° C [2]. Above this temperature, microcrystals appear in the layer [1, 5].

An empirical procedure [2] has shown that a filling coefficient, τ, could be an adequate tool for describing the general aspect of the amorphous structure; the filling coefficient was defined [2] as the ratio of the area of clusters (on micrographs) to the total area of the layer (Fig. 1); τ is practically independent from the ageing temperature up to 450° C but slowly varies with film thickness [2] (Fig. 2). Hence the parameter $\tau(d)$ may be used as a tool for describing an amorphous layer of given thickness, d, whatever be the ageing temperature (within the limit $T_R \leqq 450°$ C) [2].

The aim of this paper is to propose an interpretation for the variations in the film resistivity, ϱ_f, and its temperature coefficient, β_f, with film thickness, d, starting from the observed variations in $\tau(d)$ [2] and the set of detailed crystallographic data published in the past [1, 5 6].

Since the electronic transport properties of chemically deposited amorphous layers differ from those prepared by other technological procedures [6–8] the technical data related to chemical deposition are briefly summarized.

2. Experimental procedures

2.1. The deposition procedure [1]

The chemical deposition procedure is based on the fact that alkaline hydroborides can act as strong reducers in a basic medium; nickel–boron layers are thus obtained from nickel salts. In order to obtain a $Ni_{66}B_{34}$ macroscopic composition the following typical liquid bath is used [1]: $Ni(CH_3CO_2)_2$, NH_4OH (reaction moderator), $PdCl_2$ (catalyst element) and KBH_4 disolved in NH_4OH.

The thickness of the layer deposited on a glass substrate is a linear function of the deposition time at a rate of about 10 nm min^{-1} [1, 2]; a continuous layer is obtained for film thicknesses greater than 45 nm. The layer composition is found from nickel and boron quantitative analyses; a usual procedure is used in the case of nickel [9, 10] and a special procedure, implementing carminic acid, is used in the case of boron [1, 11], leads to an experimental inaccuracy of less than 3% [11].

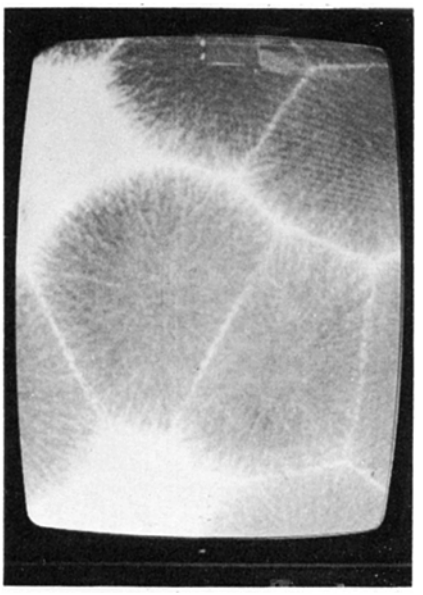

Figure 1 Electronic micrograph of unannealed $Ni_{66}B_{34}$ layer.

0022–2461/86 $03.00 + .12

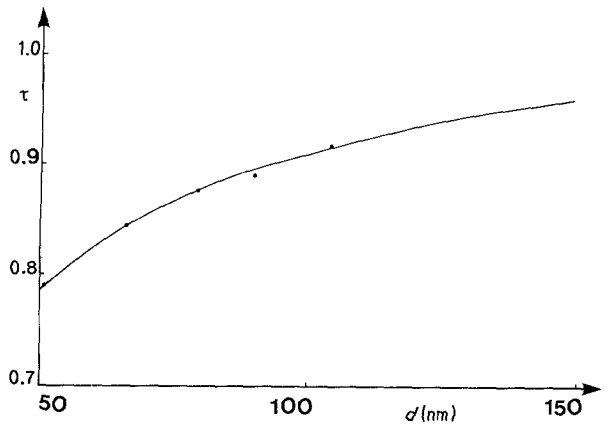

Figure 2 Variations in the "filling coefficient", τ, with film thickness d (Kuhnast *et al.* [2]).

2.2. Measurement procedures

The layers have been submitted to isothermal treatments at ageing temperature T_R, in order that the electrical parameters exhibit a stabilized behaviour [1, 2].

Programmed isothermal annealing and linear growth in temperature have been used [1, 12, 13] for analysing the evolution in the resistivity and its temperature coefficient both in the amorphous state and the crystallized state, including the relaxation domain [8].

For convenience, the effect of thermal treatment on the electrical properties was marked with an evolution coefficient, $C^{\circ}_{R_i}$, defined by [1]

$$C^{\circ}_{R_i} = [(R^{\circ}_{f,i} - R^{\circ}_{f,i+1})/R^{\circ}_{f,i+1}(T_{R,i+1} - T_{R,i})] \quad (1)$$

where $R^{\circ}_{f,j}$ is the resistance of the layer at 0° C after thermal treatment at $T_{R,j}$. The typical aspect of the variations in C°_{Ri} clearly give rough indications on the successive behaviours of the layer, as shown in Fig. 3.

2.3. Structure model

It is now generally considered [6, 8, 14] that the structure of chemically deposited amorphous layers can be described by a bidimensional array of clusters embedded in a poorly conducting medium [6, 15, 16] in the way suggested by Machizaud and co-workers [17, 18].

Such a structural model allows an interpretation of experimental data related to chemically deposited amorphous layers of nickel–phosphorus [19, 20].

In this way the structure of Ni–B layers containing 66% nickel atoms and 34% boron atoms can be regarded as cylindrical clusters, partially joined (Fig. 4). the clusters are built in conducting fibres and an external coating [1, 6, 20], as image treatment [21] clearly shows Fig. 5; the biphasic state has been identified as Ni_3B fibres and an amorphous phase [1, 5]. The amorphous phase is the cluster coating and also acts as a grain boundary (Fig. 6) [4]; moreover its thickness seems practically constant.

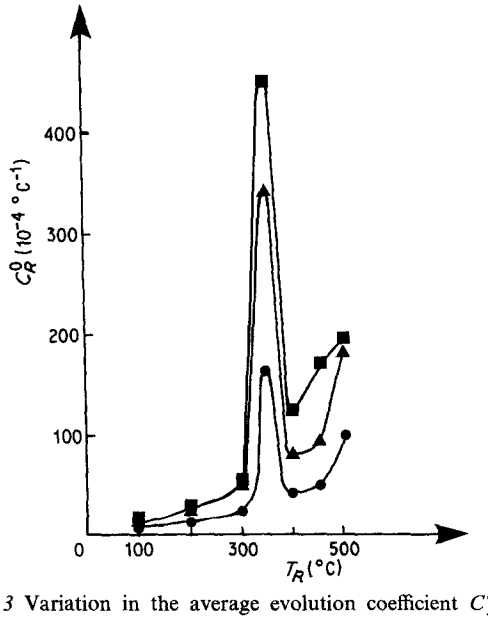

Figure 3 Variation in the average evolution coefficient C°_{R} with ageing temperature, T_R, for several film thicknesses: ■ = 66 nm; ▲ = 93 nm; ● = 158 nm (Kuhnast [1]).

3. The conduction model

3.1. Experimental features

In the whole domain of temperatures where the clusters can be clearly identified, i.e. for $T_R < 350°$ C, the experimental variations with thickness, d, in the electrical resistivity, ϱ_f, and reciprocal temperature coefficient, β_f^{-1}, can be drawn with respect to the parameter $\{1 - [\tau(d)]^{1/2}\}$ (Figs. 7 to 9). Linear plots are obtained at any ageing temperature and the slopes take decreasing values as the ageing temperature T_R becomes higher. In the case of β_f^{-1} the experimental points are scattered for $T_R = 200°$ C whereas linear plots are clearly obtained for $T_R = 100°$ C and $T_R = 300°$ C.

3.2. Interpreting the variations in the resisitivity

Since the filling coefficient $\tau(d)$ takes values near unity [2] we assume that any longitudinal electron path takes a length equal to that of the layer (Fig. 4). Since the value of $\tau(d)$ varies slightly from a given area of film to another [7, 22], due to the homogeneity of chemical layers [7], we further assume that the electron path can be statistically described in two parts: the major part corresponds to travel in conducting fibres whereas the remainder corresponds to crossings of the amorphous coating.

The bidimensional homogeneity also sustains the assumption that the length, l_a, and the width, w_a, of the fibre path is proportional to the square root of the total cluster surface. Since the total cluster surface is defined from $\tau(d)$ and from the surface of the film (equal to lw, where l is the film length and w its width), we can write

$$l_a = l[\tau(d)]^{\frac{1}{2}} \quad (2)$$

$$w_a = w[\tau(d)]^{\frac{1}{2}} \quad (3)$$

If we assume that the effect of the amorphous coatings is not marked on the current lines, because they mainly act as grain boundaries, the width of the statistical path in the coating, w_e, can be regarded as equal to w_a, i.e.

$$w_e \sim w_a \quad (4)$$

With respect to the above assumptions, the length of the path in the coating, l_e, is given by

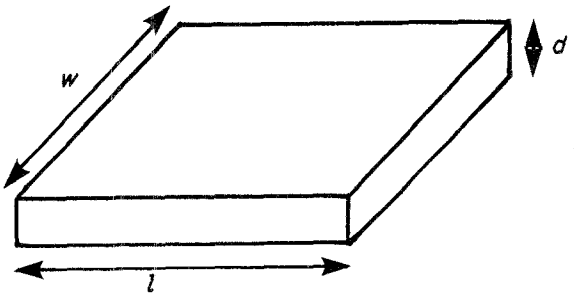

Figure 4 Model for electrical conduction, based on the macroscopic structure.

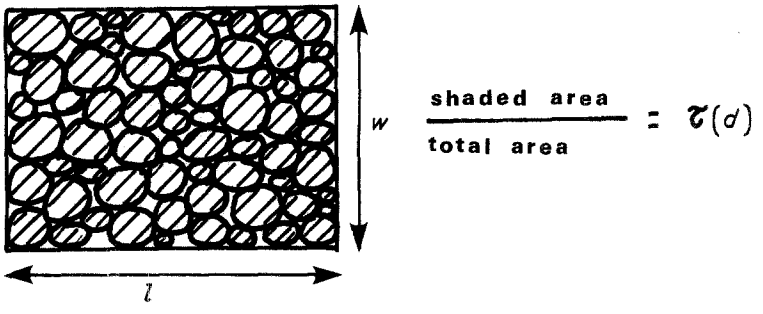

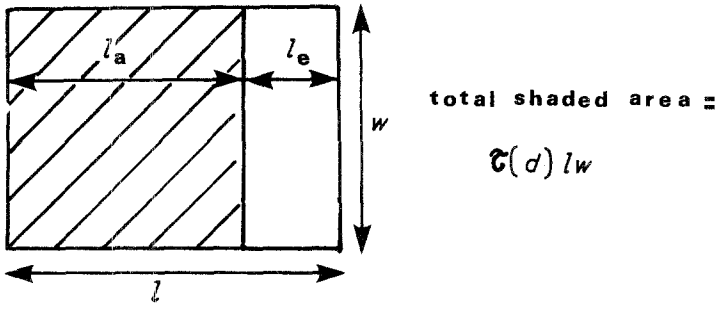

$$l_e = l - l_a = l\{1 - [\tau(d)]^{\frac{1}{2}}\} \qquad (5)$$

For a complete description of the structure it must not be forgotten that the clusters grow in a columnar fashion, whatever the film thickness [1, 5]. This is in good agreement with the existence of a bidimensional array of clusters [1, 15, 18]; consequently, the height of the clusters is taken equal to that of the film.

Finally, the film resistance, R_f, is given by

$$R_f = \left(\varrho_1 \frac{l_a}{w_a} + \varrho_2 \frac{l_e}{w_e}\right)(1/d) \qquad (6)$$

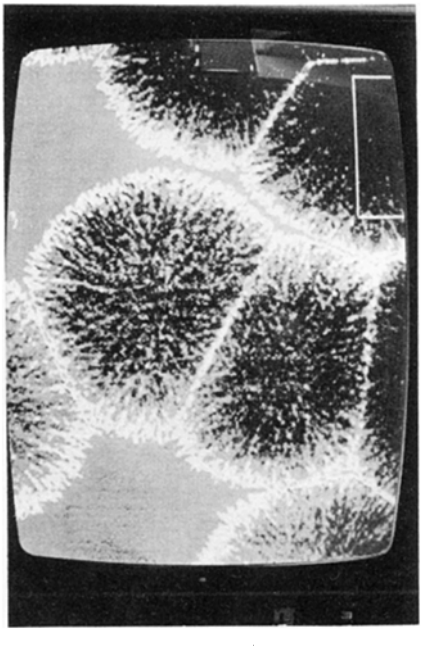

Figure 5 View of Fig. 1 under the action of an analogous image treatment showing the conducting fibres.

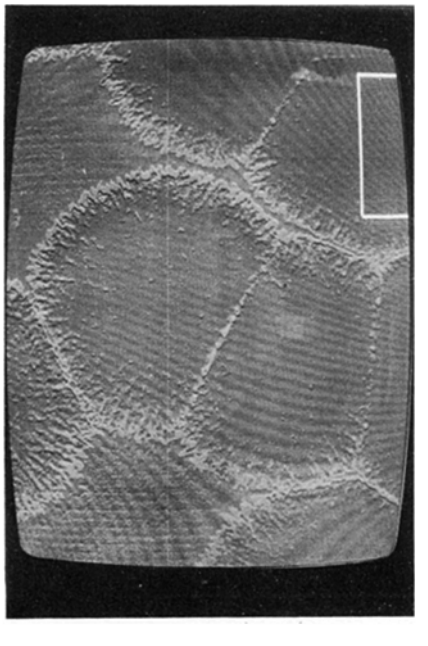

Figure 6 Cluster coating shown by a special image technique.

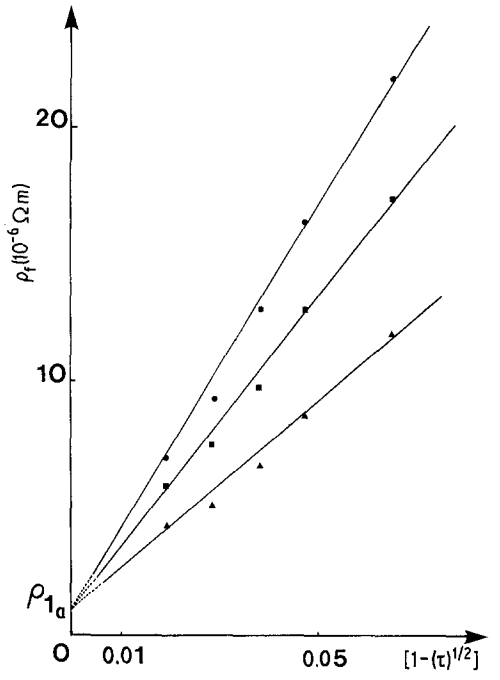

Figure 7 Variations in the film resistivity, ϱ_f, with $[1 - (\tau)^{1/2}]$ at several ageing temperatures (● = 100° C; ■ = 200° C; ▲ = 300° C).

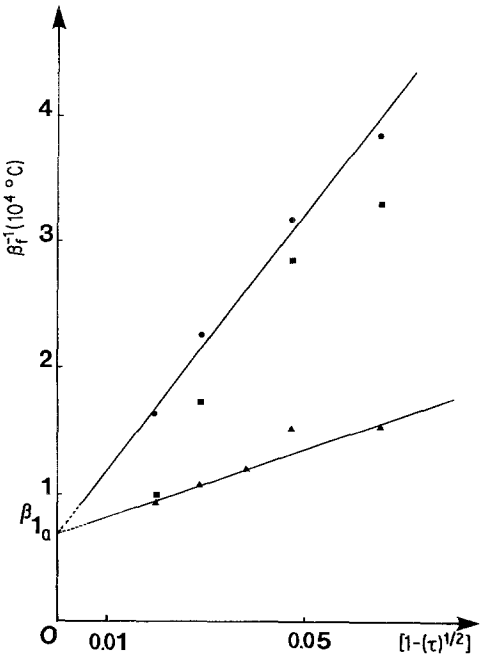

Figure 9 Variation in the reciprocal film tcr β_f^{-1}, with $[1 - (\tau)^{1/2}]$ at several ageing temperatures (● = 100° C; ■ = 200° C; ▲ = 300° C).

where ϱ_1 is the resistivity of the fibre and ϱ_2 the resistivity of the coating.

Defining the apparent resistivity of the film material, ϱ_f, by the equation

$$R_f = \varrho_f \frac{l}{wd} \tag{7}$$

and taking into account Equations 2 and 7 gives

$$\varrho_f = \varrho_1 + \varrho_2 \frac{\{1 - [\tau(d)]^{\frac{1}{2}}\}}{[\tau(d)]^{\frac{1}{2}}} \tag{8}$$

this leads to

$$\varrho_f \sim \varrho_1 + \varrho_2\{1 - [\tau(d)]^{\frac{1}{2}}\}, \quad 1 - [\tau(d)]^{\frac{1}{2}} \ll 1 \tag{9}$$

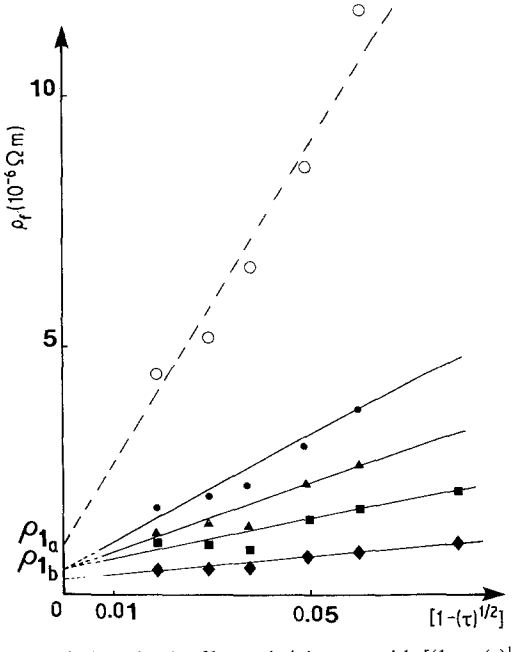

Figure 8 Variations in the film resistivity, ϱ_f, with $[(1 - (\tau)^{1/2}]$ at several ageing temperatures (0 = 300° C; ● = 350° C; ▲ = 400° C; ■ = 450° C; ♦ = 500° C).

The above equation is in fairly good agreement with experimental data (Fig. 7) assuming that ϱ_2 varies with T_R.

Defining the temperature coefficient of resistivity (tcr) β, by the usual relation [3]

$$\beta = \frac{d\ln\varrho}{dT}$$

where ϱ is the resistivity and T the temperature, a logarithmic differentiation of this equation yields

$$\beta_f\varrho_f = \beta_1\varrho_1 + \beta_2\varrho_2\left\{\frac{1}{[\tau(d)]^{\frac{1}{2}}} - 1\right\} \tag{10}$$

Provided that

$$\frac{\beta_2\varrho_2}{\beta_1\varrho_1}\left\{\frac{1}{[\tau(d)]^{\frac{1}{2}}} - 1\right\} \ll 1 \tag{11}$$

Equation 10 now becomes

$$\beta_f\varrho_f \sim \beta_1\varrho_1 \tag{12}$$

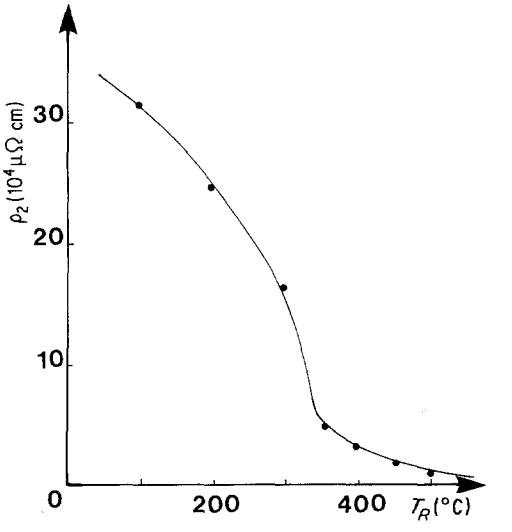

Figure 10 Variation in the resistivity ϱ_2 with ageing temperature T_R.

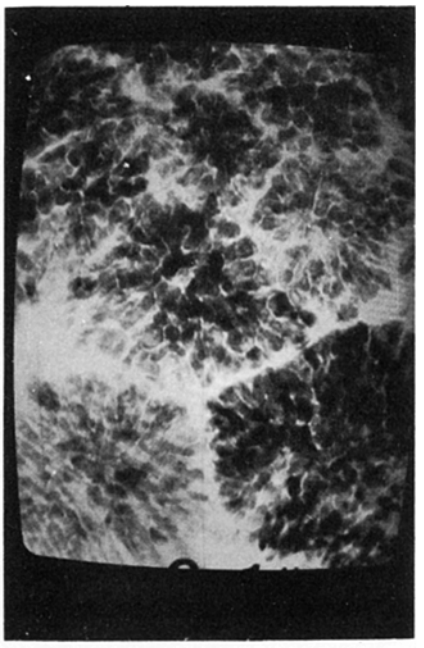

Figure 11 Electron micrograph of $Ni_{66}B_{34}$ layer annealed at 300° C for 5 h.

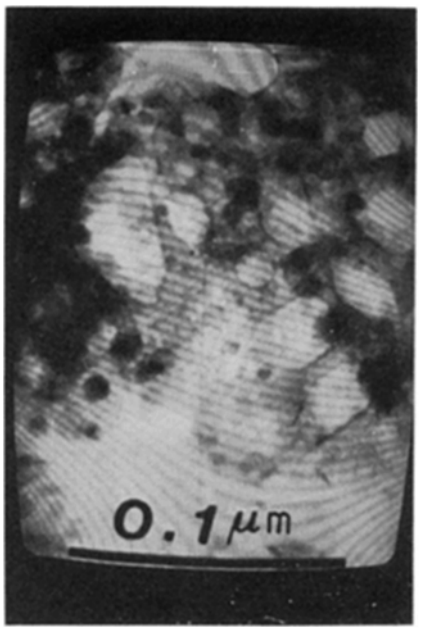

Figure 13 Electron micrograph of $Ni_{66}B_{34}$ layer annealed at 500° C for 5 h.

Hence, from Equations 9 and 12

$$\beta_f^{-1} \sim \beta_1^{-1}\left(1 + \frac{\varrho_2}{\varrho_1}\{1 - [\tau(d)]^{\frac{1}{2}}\}\right) \qquad (13)$$

in good agreement with experimental results (Fig. 9).

3.3. Analysing irreversible shifts in resistivity

From irreversible shifts in the resistivity with ageing temperature T_R (Fig. 10), three domains of temperatures must be examined; from 20 to 325° C, from 325 to 475° C and above 475° C [1]. The two last domains correspond to the relaxation domain [8].

(a) 20° C < T_R < 325° C: plots of ϱ_f against $\{1 - [\tau(d)]^{1/2}\}$ give the same asymptotic value of ϱ_f, ϱ_{1a}, for $\tau(d) = 1$, whereas the slope of the linear plots decreases for increasing values of T_R (Fig. 7). We then assume that the material of the conducting fibre takes a constant value of resistivity and we identify ϱ_1 with ϱ_{1a} in this structural state. This assumption is sustained by the fact that the X-ray scattering patterns are not modified up to T_R = 275° C [1, 5, 18]; the wide rings are unaltered. The evolution coefficient varies slightly (Fig. 3); the activation energy of the resistivity exhibits a similar behaviour as observed from differential thermal analysis (DTA) [1, 13]. When T_R takes values between 275 and 300° C, typical "hills" appear in the scattering patterns [1, 5]; the first one is situated before the first ring, attributed to strong Ni_7B_3 reflections and the second one is situated before the second ring, attributed to Ni_3B and Ni_7B_3 reflections [1, 5]. These distortions suggest modifications in the short range order and concern the coating. This prediction is in good agreement with the decrease in ϱ_2 with T_R (Fig. 10) which is more accentuated at 300° C. It is clear that the substitution of Ni_7B_3 to the coating material induces a decrease in ϱ_2. At 300° C, a very slight ray, due to Ni_3B, appears in the X-ray patterns [1, 5] and gives an insight into the evolution.

Figure 12 Image treatment of Fig. 11 revealing the grain shape.

(b) 300° C < T_R < 450° C: curves ϱ_f, $\{1 - [\tau(d)]^{1/2}\}$ converge for $\tau(d) = 1$; the obtained value of ϱ_f, ϱ_{1_b}, is lower than ϱ_{1_a} (Fig. 8). In this temperature range the rays related to the precrystallization state of Ni_3B are accentuated in the diffraction pattern [1, 2]. From the width of half-height of this ray at 350° C can be derived an approximate value of 8 nm for the mean crystallite [1], in good agreement with the size of the grains situated within the clusters (Figs. 11 and 12): As previously suggested [6] the crystallization of Ni_3B modifies the short distance order and justifies the shift from ϱ_{1_a} to ϱ_{1_b}. Above 400° C Ni_2B precipitates from a residual phase endowed with boron [1, 6] that induces a decrease in ϱ_2.

(c) $T_R \geqq$ 475° C: the amorphous progressively vanishes: rays appear in the diffraction pattern; the grain boundaries progressively disappear above 400° C and vanish at 500° C (Fig. 13) [1, 5]: The layer then exhibits a crystallized behaviour [1, 2]: the Ni_7B_3

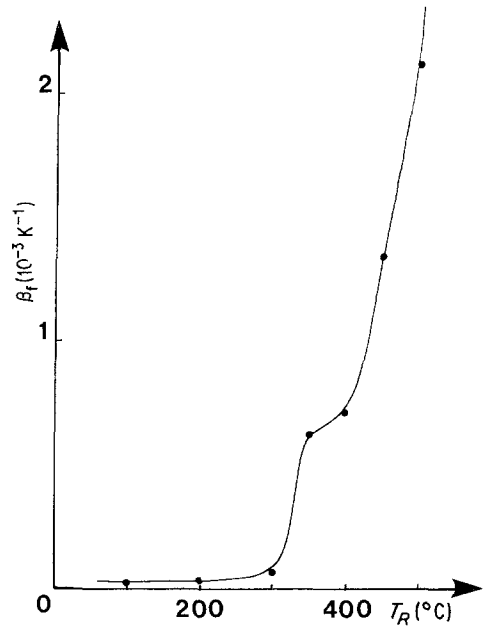

Figure 14 Variation in the film tcr β_f with ageing temperature T_R for a film thickness of 66 nm (Kuhnast [1]).

phase splits up and Ni_2B precipitates [1, 5]; a consequence is the decrease in ϱ_1. The marked decrease in ϱ_2 at 500° C is attributed to the coalescence procedure which occurs at this temperature (Fig. 13).

More generally the behaviours of the resistivity and the tcr show the same transition temperature (Figs. 10 and 14). Since the relation

$$\beta_f \varrho_f \sim \beta_{Ni} \varrho_{Ni} \qquad d > 10^2 \text{nm} \tag{14}$$

as seen in Fig. 15 where the index Ni is related to bulk nickel is verified [2] and taking into account Equation 12 we assume that conduction occurs through nickel paths in the fibres.

The following relation is then derived

$$\beta_1 \varrho_1 \approx \beta_{Ni} \varrho_{Ni} \tag{15}$$

and can be rewritten as

$$\frac{d\varrho_1}{dT} \approx \frac{d\varrho_{Ni}}{dT} \tag{16}$$

Hence

$$\varrho_1 \approx \varrho_{Ni} + \varrho_{Ni} F(q_i) \tag{17}$$

where F is an unknown function of the unknown variable q_i satisfying the relation

$$\frac{d}{dT}(\varrho_{Ni} F(q_i)) = 0 \tag{18}$$

This relation shows that q_i cannot only be a geometrical parameter, because its thermal variations would be negligible as usual [4] and Relation 18 would unsatisfied.

Equation 18 can be rewritten as follows

$$\frac{d \ln \varrho_{Ni}}{dT} + \frac{d \ln F(q_i)}{dT} = 0 \tag{19}$$

that suggests to implement the new function G

$$F(q_i) = \lambda_0 G(q_i) \tag{20}$$

where λ_0 is mean free path in the bulk material and

$$\frac{dq_i}{dT} = 0 \tag{21}$$

Equation 17 then becomes

$$\varrho_1 = \varrho_{Ni}[1 + \lambda_0 G(q_i)] \tag{22}$$

This equation could correspond to a linearized expression related either to the Fuchs– Sondheimer effect [3, 4], or to grain boundary scattering [4], or to both effects [4].

It is clear that an effect similar to the grain boundary scattering is due to the coating but no evidence exists for a Fuchs–Sondheimer effect in the fibres, because it cannot be established that the fibre diameter is of the same order of magnitude as the bulk electron mean free path.

The fact that a statistical description of the electronic conduction seems satisfactory is not surprising since it is known that this type of amorphous layer prepared by chemical reactions [1, 10, 17, 23] (or by an electrochemical procedure [24, 25]) exhibits short range order due to the clusters and high distance order due to the array of clusters [6].

The proposed model differs from those used by most other workers [26–28] in the case of metal/metalloid layers but no agreement with experimental results has been obtained, except at low temperature [27] or in experimental conditions [29], where the theoretical expressions of Ziman seem inadequate [16]. Moreover, the structure parameters are derived from the dense random packing of hard spheres, DRPHS, theory [8] which does not allow a firmly based description of this type of amorphous layers, as pointed out by several workers [6, 8, 14, 30]; the main criticism concerns the assumed homogeneity which is in contradiction with experimental results. The models proposed by Boudreaux [31] and Gaskell [32] and Machizaud [6, 20] seem more adequate [8].

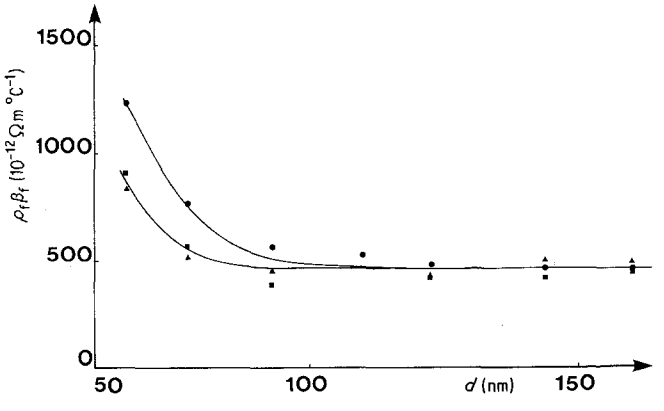

Figure 15 Variations in the product of the film resistivity with the tcr $\varrho_f\beta_f$, with the film thickness, d, the ageing temperature T_R acting as a parameter (▲ = 100° C; ■ = 200° C; ● = 300° C; Kuhnast *et al.* [2]).

4. Conclusions

Assuming that the amorphous layer of $Ni_{66}B_{34}$, chemically deposited, can be represented by a bi-dimensional array of clusters, partially joined and separated by a thin, poorly conducting coating, one can qualitatively interpret the variations in the resistivity and its tcr with thickness and ageing temperature.

Acknowledgements

Thanks are due to the French Ministry of Industry and Research for financial support (contract CP 81-1-C 742).

References

1. F. A. KUHNAST, thèse Université de Nancy (1979).
2. F. A. KUHNAST, F. MACHIZAUD, J. FLECHON, C. R. PICHARD and A. J. TOSSER, *Thin Solid Films* **81** (1981) 181.
3. E. H. SONDHEIMER, *Adv. Phys.* **1** (1952) 1.
4. C. R. TELLIER and A. J. TOSSER, "Size effects in thin films" (Elsevier, Amsterdam, 1982) Chapt. 1.
5. F. A. KUHNAST, F. MACHIZAUD, R. VANGELISTI and J. FLECHON, *Microsc. Spectros. Electron* **4** (1979) 553.
6. F. MACHIZAUD, F. A. KUHNAST, G. MBEMBA and J. FLECHON, *J. Phys. C* **9** (1982) 75.
7. C. R. PICHARD, A. J. TOSSER, M. BEDDA, F. A. KUHNAST, F. MACHIZAUD, J. FLECHON, Coll. Matériaux, 1984 PIRMAT- CNRS, Paris (28-30 mai 1984) – poster.
8. Ph. MANGIN, "Les amorphes métalliques" (Ecole d'Hiver d'Aussois, éd. de Physique, Paris, 1983) p. 272.
9. G. CHARLOT, "Chimie analytique quantitative", 6th edition, Vols 1 and 2, (Masson and Son, 1974).
10. J. FLECHON, thèse, Université de Nancy (1960).
11. J. FLECHON and F. A. KUHNAST, *Bull. Soc. Chim. Fr.* **56** (1976) 739.
12. J. FLECHON, F. A. KUHNAST and F. MACHIZAUD, *Thin Solid Films* **52** (1978) 89.
13. J. FLECHON, F. A. KUHNAST, F. MACHIZAUD, B. AUGUIN and A. DEFRESNE, *J. Phys.* **42** (1981) 97.
14. J. BLETRY, *Rev. Phys. Appl.* **15** (1980) 1019.
15. E. BELIN, C. BONNELLE, J. FLECHON and F. MACHIZAUD, *J. Non-Cryst. Solids* **41** (1980) 219.
16. J. RIVORY, "Les amorphes métalliques (Ecole d'Hiver d'Aussois, éd. de Physique, Paris, 1983) p. 512.
17. F. MACHIZAUD, Thèse, Université de Nancy (1973).
18. F. MACHIZAUD, F. A. KUHNAST and J. FLECHON, *J. Phys., Coll.* **4** Suppl. 36, 83.
19. C. R. PICHARD, A. R. ES SLASSI, A. J. TOSSER and F. MACHIZAUD, *Thin Solid Films* **112** (1984) 289.
20. F. MACHIZAUD, F. A. KUHNAST and J. FLECHON, *J. Non-Cryst. Solids* **68** (1984) 271.
21. C. OHUCHI, P. MAGNETTE, A. DELORME, J. MASSON, F. SOEHNLEN and A. J. TOSSER, IASTED Congress MIC February 84, Innsbrück, Proceedings *Acta Press* (1984) 63.
22. A. J. TOSSER, C. R. PICHARD, M. ZANTOUT, M. BEDDA and J. FLECHON, IASTED Congress MIC February 84, Innsbrück, Proceedings *Acta Press* (1984) 164.
23. J. FLECHON, S. KARBAL and G. MBEMBA, *J. Chimie* (1985) in press.
24. A. RASHID, thèse de Spécialité, Université de Nancy (1983).
25. A. OBAIDA, thèse de Spécialité, Université de Nancy (1983).
26. P. J. COTE and L. V. MEISEL, "Glassy Metals I, Topics in Applied Physics 46" (Springer Verlag, Berlin, 1981) p. 141.
27. K. FROBOSE and J. JAECKLE, *J. Phys. F* **7** (1977) 233.
28. J. HAFNER, E. GRATZ and H. J. GUNTHERODT, *J. Phys. Coll. C8* **41** (1980) 512.
29. S. J. NAJEL, J. VASSILIOU, P. M. HORN and B. C. GIESSON, *Phys. Rev. B* **17** (1978) 462.
30. C. R. PICHARD, Z. BOUHALA, A. J. TOSSER, A. RACHID and J. FLECHON, *J. Mater. Sci.* (1985) in press.
31. D. S. BOURDEAUX and J. M. GREGORD, *J. Appl. Phys.* **48** 152.
32. P. H. GASKELL, *J. Non-Cryst. Solid.* **32** (1979) 207.

Received 19 February
and accepted 13 March 1985